

Simulation of ion trajectories through the mass filter of a quadrupole mass spectrometer

F.M. Ma
S. Taylor

Indexing terms: Quadrupole mass spectrometer, Ion trajectory simulation

Abstract: The paper describes the development of a computer program designed to simulate the performance of the mass filter in an ideal quadrupole mass spectrometer (QMS). The simulation program provides flexible input parameters to allow the user to investigate the ion trajectories and transmission efficiency for different operating conditions. The program is used to analyse the change in QMS resolution with the number of RF cycles, DC voltage, RF voltage magnitude and phase angle. The angle at which ions enter the mass filter is shown to be significant and the effect of RF phase on transmission probability through the filter is seen to be critical. A comparison of the simulation with experimental QMS results shows excellent agreement.

1 Introduction

Quadrupole mass spectrometers are widely used both in research laboratories and in industry, where accurate scientific data can be obtained for many surface studies in vacuum systems. An example is residual gas analysis (RGA) in a semiconductor device fabrication plant. There are also many important uses for the QMS in the chemical industry for the analysis of simple and complex molecules, particularly when used in conjunction with gas chromatography. These varied applications have many different requirements for resolution, sensitivity, stability etc.

A description of quadrupole mass spectrometer (QMS) construction and operation is available in the scientific literature [1,2] and will not be repeated here. The QMS consists primarily of the following three separate components: (i) ion source, (ii) mass filter and (iii) ion detector. Although much experimental work is reported in the literature [3], detailed models of the QMS mass filter are lacking. The theoretical analysis of the mass filter involves the solution of the Mathieu equation under special boundary conditions. The most comprehensive treatment available is that of Dawson [2], who solved the Mathieu equation in two dimensions for an infinitely long mass filter. This work was

further developed by Batey [3] to include a presentation of the ion stability diagram. In an earlier work [4], Dawson used matrix methods to calculate ion transmission based on maximum ion displacements for mass filters of both infinite and finite length. However, due to the time consuming nature of the numerical calculations involved, a real time simulation of ion trajectories for large numbers of ions successively admitted into the filter has not seriously been attempted before. The need remains therefore for such a theoretical model to simulate QMS performance for a range of operating conditions. An important advantage of such a numerical approach over earlier analytical techniques is that it becomes possible to consider the effects of changes in filter length on performance. This is most important in practice, since in so many applications relatively short filters are used and the operation is very far from the ideal. The data obtained in this analysis are presented in terms of the number of RF cycles (N) to which ions are subject in the filter rather than the actual length. Thus the effect of increasing N from 50 to 100 (say) can be achieved by either (a) increasing the length of the filter by a factor of 2 or (b) increasing the RF frequency by a factor of 2 or (c) reducing the velocity of the ions in the axial (z -) direction by a factor of 2.

2 Theory

The mass filter in a QMS operates as a dynamic mass analyser by causing ions of different charge to mass ratio to follow different trajectories by the application of alternating and direct electromagnetic fields.

Following Dawson [2], the potential distribution inside an ideal mass filter with hyperbolic electrodes is given by

$$\phi(x, y, z) = \phi_0 \left(\frac{x^2 - y^2}{2r_0^2} \right) \quad (1)$$

where r_0 is the radius of the filter. This distribution may be set up to a good approximation by the use of cylindrical electrodes, which is the usual case in practice. The distribution satisfies the Laplace equation and is invariant in the z -direction.

Consider the motion of an ion of mass m and charge e subject to the electric field E defined by eqn. 1. The motion of an ion in the x - and y -directions depends on the variation with time of the potential ϕ_0 . For the ideal mass filter operation, a combination of direct (U) and alternating voltages (V) is chosen and applied to opposite rods such that:

$$\phi_0 = U - V \cos(2\pi ft) \quad (2)$$

where f is the frequency and t is the time. Hence, three

independent differential equations of motion are obtained:

$$E_x = -(U - V \cos \omega t) \frac{x}{r_0^2} \quad (3)$$

$$E_y = -(U - V \cos \omega t) \frac{y}{r_0^2} \quad (4)$$

$$E_z = 0 \quad (5)$$

Considering only the x - and y -directions, by substituting the terms m , r_0 , f , U and V by \mathbf{a} and \mathbf{q} , the following equations are obtained:

$$a_u = a_x = -a_y = \frac{4eU}{m\omega^2 r_0^2} \quad (6)$$

$$q_u = q_x = -q_y = \frac{2eV}{m\omega^2 r_0^2} \quad (7)$$

If time is expressed in terms of the parameter ξ , where $\xi = \omega t/2$, eqns. 6 and 7 can be expressed as an equation of motion in the general form of the Mathieu equation:

$$\frac{d^2 u}{d\xi^2} + (a_u - 2q_u \cos 2\xi)u = 0 \quad (8)$$

where u represents either x or y .

From eqn. 8, it can be seen that the trajectory depends on the phase angle at which the ion enters the field. Solving the equation, the position of the ion at any time instant can be determined. If the ion experiences an obstruction-free path over the defined N , it is said to be stable within this length. Conversely an unstable ion can be described as an ion which makes contact with either of the electrode rods. This establishes the fundamental principle of the analysis.

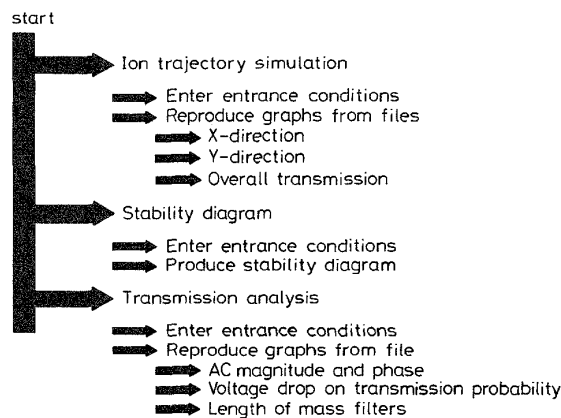


Fig. 1 Tree diagram for simulation program

3 Software details

3.1 Program structure

The program was written in turbo-PASCAL and runs under DOS on any PC with a VGA monitor. The program is fully menu driven with a menu breadth of six and maximum menu depth of three. The entire program suite is over 2000 lines long including error handling and data handling routines, and a tree diagram showing the organisation is given in Fig. 1. The suite can be divided into three parts, as follows:

- (i) ion trajectory determination
- (ii) generation of Mathieu stability diagram
- (iii) transmission analysis.

Each of the above options can be accessed independently and data files generated. The program allows the reproduction of graphs using data already in files. Separate filenames can be used to keep a record of results obtained, and thus allow the construction of a database for a particular QMS design and/or mode of operation.

3.2 Ion trajectory simulation

The program uses a fourth-order Runge-Kutta numerical approximation to solve eqn. 8 and the algorithm for this calculation is given in the Appendix. The input operating conditions which may be varied by the user include ion mass, ion velocity and position in the x - y plane at the entrance to the mass filter, RF phase angle and frequency, direct voltage (U) and alternating voltage (V) magnitudes, number of RF cycles and r_0 . Fig. 2 shows the trajectory in the x -direction for an ion of mass 28 atomic mass units (a.m.u), over 50 cycles of the RF waveform. The radius of the mass filter is 2.75 mm and is shown as a dotted line on the diagram. Clearly the displacement in x at no point exceeds 2mm and thus the ion is said to be stable in x . Similarly, Fig. 3 shows an example of a stable ion trajectory in the y -direction over 100 RF cycles.

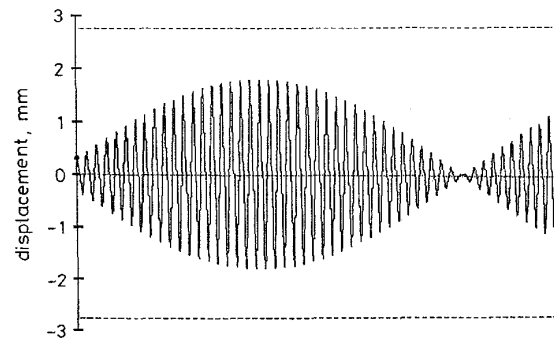


Fig. 2 Ion displacement as a function of number of RF cycles showing stable ion trajectories through mass filter in x -direction. Initial values of x (x_0) and y (y_0) = 0.3mm; initial entrance velocity (u_0) = 0; phase = 45°; U = 20 V; V = 123.5V

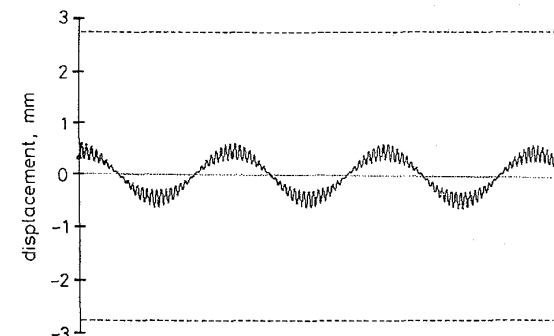


Fig. 3 Ion displacement as a function of number of RF cycles showing stable ion trajectories through mass filter in y -direction. Initial values of x (x_0) and y (y_0) = 0.3mm; initial entrance velocity (u_0) = 0;

3.3 Stability diagram

The ideal stability diagram, also known as the Mathieu diagram, is used to show the conditions for simultaneous stability in both x - and y -directions for an infinitely long filter. The area bounded by the curves is called the 'stability triangle' and represents the values of U and V (or a and q) for which the ion displacement in x and y is less than r_0 .

After Dawson [2], it is possible to use the tip of the stability region to obtain mass resolution for an infinitely long filter. All ions of the same mass to charge ratio have the same operating point on the stability diagram for fixed values of r_0 , phase, U and V . In order to generate a mass spectrum, V is scanned, with U following it, so that U and V follow a locus or mass scan line. This line represents ions of constant U to V ratio and passes through the origin of the stability diagram. A particular mass is transmitted through the filter only if U and V lie within the stability region for that particular mass. Ions of lower mass will be unstable in the x -direction while ions of higher mass unstable in the y -direction. Fig. 4 shows the stability diagram and scan line for critical mass 28 a.m.u. (i.e. the ion is a singly charged nitrogen molecule). Also shown dotted is the stability diagram for mass 14 (i.e. a singly charged nitrogen atom).

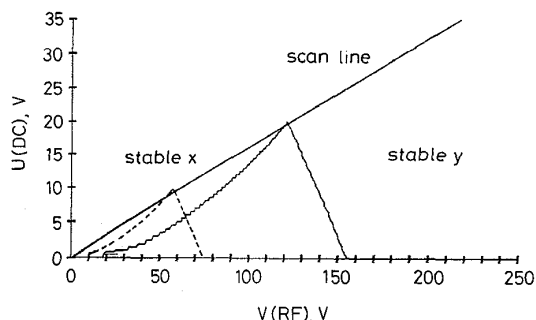


Fig. 4 Stability diagram showing peak condition for nitrogen (N_2^+) at $U = 20V$ and $V = 123.5V$. Filter radius (r_0) = 2.75 mm and frequency (f) = 2 MHz

Two of the attractive features of the QMS are thus seen:

- (i) the resolution can be varied electronically by adjustment of the U/V ratio
- (ii) there is a simple linear relationship between the mass number of the species transmitted and the magnitude of the applied voltages U or V . The mass scale is linearly related to V . This enables the identification of unknown peaks and allows selective multipeak monitoring.

Using the program the stability of a particular ion entering the mass filter can be determined and the QMS resolution for a particular set of operating parameters easily determined. QMS design for a particular application is thus greatly facilitated.

3.4 Transmission analysis

3.4.1 The effect of RF magnitude, phase and entrance angle on ion transmission through the mass filter: This analysis forms the main part of the whole program since no previous calculations of ion transmission by successive determination of ion trajectories has been reported to the authors' knowledge to date. This is achieved by injecting a relatively large number of ions (e.g 100 – 5000) into the mass filter and calculating the ion trajectories in x and y in each case as one of the operating conditions is continuously varied. For example Figs. 5–7 show the transmission analysis for 360 ions of mass 28 injected into the mass filter described in Section 3.2 ($f = 2\text{MHz}$, $r_0 = 2.75\text{mm}$) under the same RF and direct voltage magnitudes. The difference is that for successive ions the RF phase angle

(i.e. point-on-wave at ion injection) was increased by 1° in each case. Fig. 5 shows the percentage of the distance travelled along the mass filter in the x -direction as ions are injected with different values of phase angle, Fig. 6 shows the same information for ion trajectories in the y -direction and Fig. 7 shows the total number of ions transmitted (i.e. successfully travelling through the filter, for both x - and y -directions).

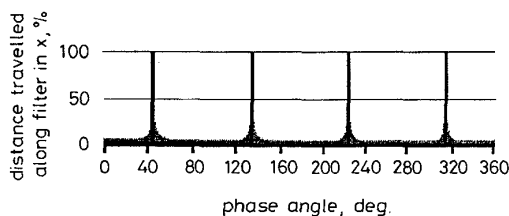


Fig. 5 Ion transmission through filter in x -direction as RF phase varies from 0° to 360° . $x_0 = y_0 = 0.3\text{mm}$; $u_0 = 0\text{m/s}$; $U = 20V$; $V = 123.5V$; and number of RF cycles $N = 100$

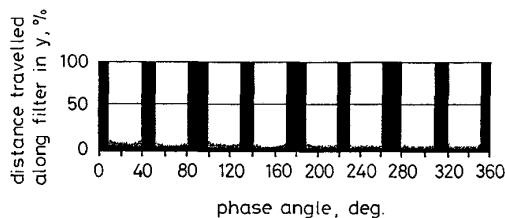


Fig. 6 Ion transmission through filter in y -direction as RF phase varies from 0° to 360° . $x_0 = y_0 = 0.3\text{mm}$; $u_0 = 0\text{m/s}$; $U = 20V$; $V = 123.5V$; and number of RF cycles $N = 100$

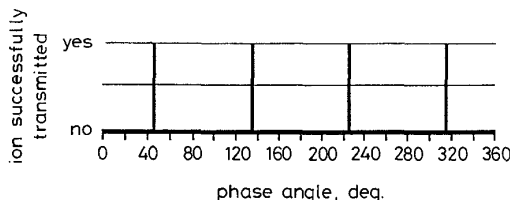


Fig. 7 Ion transmission through filter in x - and y -direction as RF phase varies from 0° to 360° . $x_0 = y_0 = 0.3\text{mm}$; $u_0 = 0\text{m/s}$; $U = 20V$; $V = 123.5V$; and number of RF cycles $N = 100$

These Figures reveal a number of interesting features:

- (i) clearly the ion transmission probability and hence QMS performance depends critically upon the phase of the RF waveform at the point of injection of the ions into the mass filter
- (ii) the RF phase has a greater effect upon the ion trajectory in one direction than in the other
- (iii) ions injected at different values of RF phase which are unstable and not transmitted through the mass filter are not all equally unstable, i.e. ions at phase angle 50° (Fig. 5) travel further down the mass filter than ions injected at a phase angle of 100° . The implication of this is that shorter mass filters may allow ions to be transmitted which are outside the stability region discussed earlier (Section 3.3).

This last feature is more easily seen if the phase increment is reduced to 0.5° expanding the x -axis on Figs. 5–7 at the regions of interest. Fig. 8 shows the transmission analysis for the mass filter for three values of U and V as the phase angle varies between 80° and 100° . For Fig. 8a all ions travel completely (100%)

through the filter in the x -direction whilst in the y -direction ions travel increasing distances through the filter before becoming unstable until injected at a phase angle of 88° at which point ions are successfully transmitted.

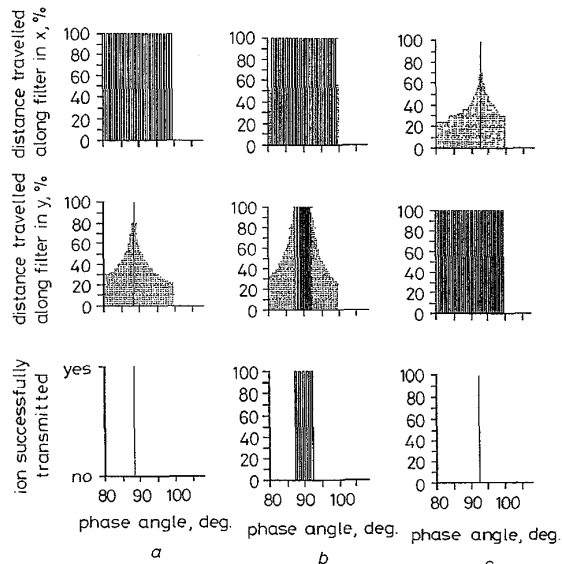


Fig. 8 Ion transmission through the filter as the RF phase varies from 80° to 100°
 $x_0 = y_0 = 0.3\text{mm}$; $u_0 = 0\text{m/s}$; $N = 25$
 a $V = 121\text{V}$, $U = 20.281\text{V}$
 b $V = 123\text{V}$, $U = 20.616\text{V}$
 c $V = 125\text{V}$, $U = 20.951\text{V}$

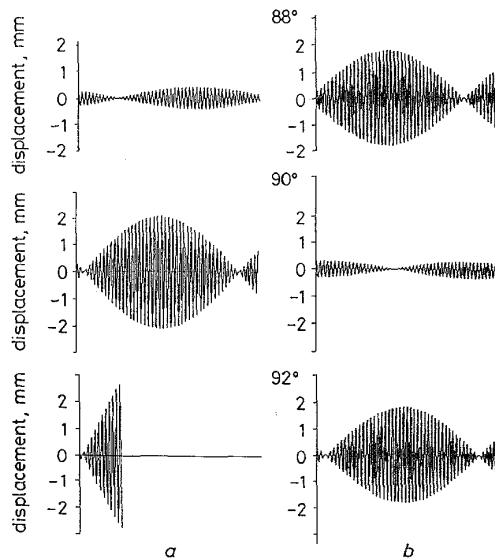


Fig. 9 Ion trajectories in x -direction for non-zero entrance angle as RF phase varies between 88° and 92°
 100 cycles
 a Nonzero entrance angle
 b Zero entrance angle

The effect of changes in U and V are also seen. Comparing Fig. 8b with Fig. 8c, as V increases more ions are successfully transmitted in the y -direction and fewer in the x -direction. The stability thus changes from stable in x to stable in y as the operating point moves up the scan line.

For each of the simulations described above ions enter the mass filter normal to the x - y plane, i.e. having zero entrance angle. The effect of altering this angle

may be conveniently simulated using the program by altering the input velocity in the x -direction with respect to the y -direction. Fig. 9 shows ion trajectories in the x -direction as the phase angle changes from 88° to 92° for two values of ion entrance angle into the filter; in Fig. 9a for an input angle of 1.6° to the filter axis and in Fig. 9b parallel to the filter axis (i.e. zero entrance angle). In Fig. 9a the trajectories become increasingly unstable as the phase angle increases. In Fig. 9b, the trajectories for the three conditions are stable. This effect clearly has implications for the design of the optics in the ion source and entrance to the mass filter and merits further investigation.

3.4.2 Effect of operating conditions on the simulated mass spectrum:

By varying V for a fixed U/V ratio a mass spectrum may be generated using the program, as shown in Fig. 10. Here 100 ions of mass 28 having zero entrance angle and velocity and a fixed spatial location in the x - y plane were injected into the mass filter at the same RF phase but with V varying between 120 to 124V in 200mV increments. The direct voltage U was kept in a constant ratio to V so that a line passing through the origin on the stability diagram shown in Fig. 4 and a point below the tip of the stability peak for mass 28 was effectively scanned. As V increases from 120V the percentage of injected ions successfully transmitted through the mass filter increases rising to a peak at $V = 122\text{V}$ and then falling sharply as V increases further. The simulation is thus generating a mass spectrum for ions injected under those conditions. Furthermore the simulation is also predicting a 'long tail' (i.e. higher transmission probability) on the low mass side of the spectrum, a condition frequently observed in practice [1]. This confirms that the experimental long tail feature is a function of the mass filter operation and not a measurement artefact. Ion transmission is also a function of entrance aperture [4] but this effect has not been considered in these simulations.

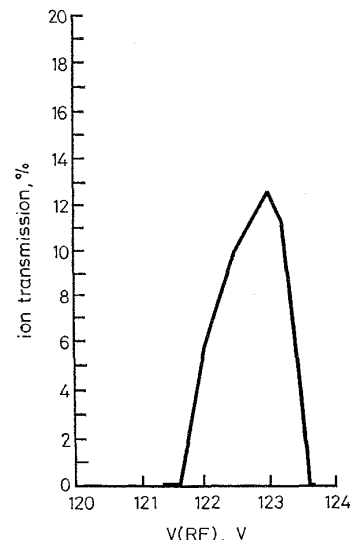


Fig. 10 Simulated mass spectrum for operating conditions and scan line for filter of Fig. 4
 100 ions injected with initial conditions $x_0 = y_0 = 0.3\text{mm}$, $u_0 = 0$, $N = 100$

The data presented in Fig. 10 for one value of U may be displayed using three dimensional axes for a range of U as shown in Fig. 11. Here the percentage of ions

transmitted, V , and the direct voltage drop below the tip of the stability diagram δU , form mutually perpendicular axes. The result that the transmission probability decreases as δU decreases (i.e. as the direct voltage is closer to the tip of the stability diagram) is clearly seen. The long tails on the low mass side of the spectrum are also apparent. The simulated spectra are broad, indicating that the resolution of the filter for these operating conditions is not particularly high, due to the low number of RF cycles experienced by the ions.

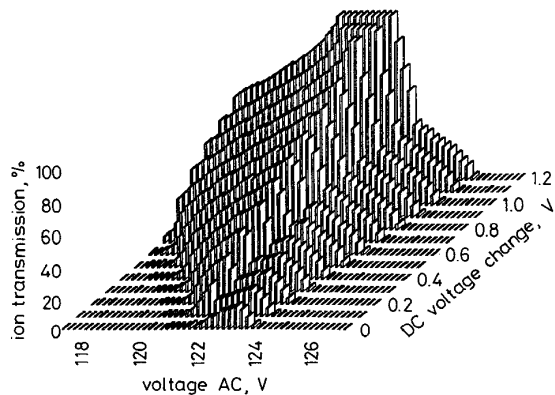


Fig. 11 Three-dimensional transmission analysis showing combined effect of δU and V on mass spectra

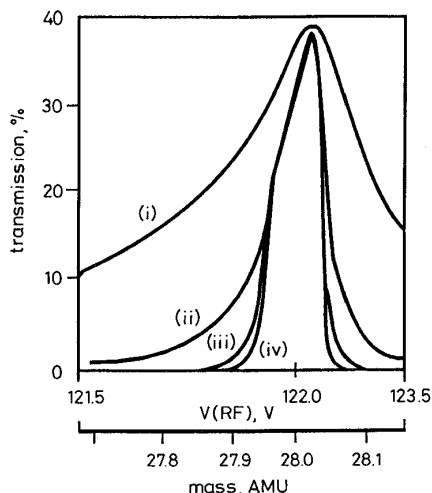


Fig. 12 Effect of number of RF cycles (N) on the mass spectra (i) 25 cycles; (ii) 50 cycles; (iii) 100 cycles; (iv) 200 and 400 cycles

3.4.3 Simulation of different length mass filters: Fig. 12 shows the effect of altering the length of the mass filter. This is achieved by obtaining mass spectra for different numbers of RF cycles (N) experienced by the ions whilst keeping the frequency of operation constant, thus effectively altering the time for which ions are subject to the filter field. These data were obtained when the operating point was taken along the scan line shown in Fig. 4. The curves illustrate graphically the importance of N in determining filter performance showing a dramatic improvement in resolution by increasing N from 25 to 50 and to 100. However the simulation showed no measurable improvement when increasing N beyond 200. Thus under these particular operating conditions $N = 200$ effectively represents an infinitely long filter. This is

particularly important as it allows the design and/or operating conditions of a mass filter to be tuned to a particular application, with consequent reduction in manufacturing costs.

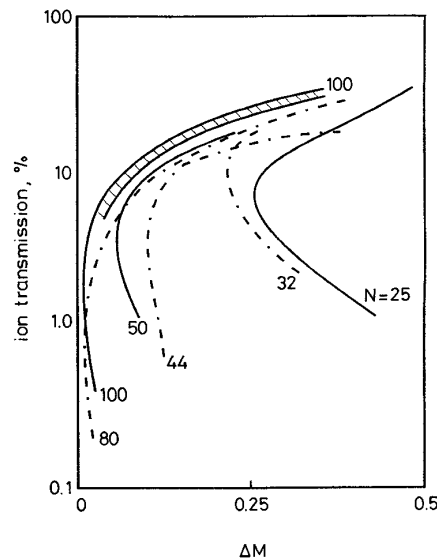


Fig. 13 Comparison between experimental and simulated QMS performance
— simulation
--- experiment

4 Comparison with experimental results

Fig. 13 shows the results obtained from a series of experiments on a real QMS, of length 125mm, constructed using circular rods 6.25mm in diameter. The results are referenced to Ar^{++} (mass 20 a.m.u.). Since the percentage of ions transmitted through a real filter cannot easily be measured the ordinate scale (% transmission) has to be normalised in a quite arbitrary fashion. The normalisation is such as to make the experimental and simulated measurements of percentage transmitted agree at approximately $\Delta M = 1.0$ a.m.u. The simulated curves for $N = 25$ and $N = 50$ cycles refer to ions injected into the filter parallel to the major axis. The results for $N = 100$ show curves for ions injected at 30° to the major axis (lower curve) as well as for ions injected parallel to the major axis (upper curve). The results show that:

- (i) the minimum ΔM achievable (maximum resolution R_{max}) increases as the number of cycles N is increased following (approximately) the relationship $R_{\text{max}} \propto N^2$
- (ii) the experimental observation that ΔM passes through a minimum as the transmission through the filter is decreased at a given N is fundamental to the quadrupole operation and is not a measurement artefact
- (iii) the entrance angle of the ions affects the overall transmission efficiency.

5 Conclusions

A flexible computer model of the mass filter in a QMS has been formulated and shown to give valuable insight into the actual behaviour of an ion under the field within the mass filter. The main original feature of the program is the ability to study the ion trajectories and thus study transmission efficiency for a finitely long

QMS under a range of operating conditions and for different design dimensions. The program accurately simulates the stability and how applied voltages affect the mass spectrum. The effect of RF phase is seen to be very critical to QMS performance. Indications that the entrance angle has a significant effect on ion transmission also have important implications for QMS design. The program accurately predicts the long tail on the low mass side of the mass spectrum observed in practice. Good agreement between simulation results and those obtained experimentally is demonstrated.

6 Acknowledgments

The authors would like to acknowledge Professor J.H. Leck for his kind and patient guidance and for a critical reading of the manuscript, W.E. Austin for his technical assistance and Dr J.H. Batey for his expert review of the results obtained.

7 References

- 1 MAO, F.M., and LECK, J.H.: 'The quadrupole mass spectrometer in practical operation', *Vacuum*, 1987, **37**, pp. 669-675
- 2 DAWSON, P.H.: 'Quadrupole mass spectrometry and its applications' (Elsevier, 1976)
- 3 BATEY, J.H.: 'Quadrupole gas analysers', *Vacuum*, 1987, **37**, pp. 659-668
- 4 DAWSON, P.H.: 'A detailed study of the quadrupole mass filter', *Int. J. Mass Spectrom. Ion Phys.*, 1974, **14**, pp. 317-337

8 Appendix: Algorithm for Runge-Kutta calculation

Considering the general first-order differential equation $dy/dx = f(x, y)$ with $y(x_0) = y_0$, the algorithm is based on the widely used formula:

$$y_1 = y_0 + (k_1 + 2k_2 + 2k_3 + k_4)/6$$

where h is the step (time) interval, $k_1 = hf(x_0, y_0)$, $k_2 = hf(x_0 + h/2, y_0 + k_1/2)$, $k_3 = hf(x_0 + h/2, y_0 + k_2/2)$, and

$k_4 = hf(x_0 + h, y_0 + k_3)$. This approach applied to eqn. 8 is coded as shown below:

```

Procedure Runge_Kutta (Var V1,VZ1,A,Q,Sign: Real);
Var K11,K12,K21,K22,K31,K32,K41,K42,T2,T3,T4,
V2,V3,V4,VZ2,VZ3,VZ4: Real;
begin
K11 := TimeInterval*VZ1;
K12 := Sign*(A+2*Sign*Q*COS(2*(NewTime+Phase-
Value*PI/180)))*V1*TimeInterval;
T2 := NewTime+TimeInterval/2;
V2 := V1+K11/2;
VZ2 := VZ1+K12/2;
K21 := TimeInterval*VZ2;
K22 := Sign*(A+2*Sign*Q*COS(2*(T2+PhaseValue*
PI/180)))*V2*TimeInterval;
T3 := NewTime+TimeInterval/2;
V3 := V1+K21/2;
VZ3 := VZ1+K22/2;
K31 := TimeInterval*VZ3;
K32 := Sign*(A+2*Sign*Q*COS(2*(T3+PhaseValue*
PI/180)))*V3*TimeInterval;
T4 := NewTime+TimeInterval;
V4 :=V1+K31;
VZ4 := VZ1+K32;
K41 := TimeInterval*VZ4;
K42 := Sign*(A+2*Sign*Q*COS(2*(T4+PhaseValue*
PI/180)))*V4*TimeInterval;
Newtime := T4;
V1 := V1+(K11+2*K21+2*K31+K41)/6;
VZ1 := VZ1+(K12+2*K22+2*K32+K42)/6;
end;

```